Lasers in Manufacturing Conference 2023

Unwanted X-ray emission in ultrashort pulse laser processing: from metallic to biological materials

Sebastian Kraft[a,b], Katrin Böttcher[a], Jörn Bonse[a], Jörg Schille[b], Udo Löschner[b], Jörg Krüger[a,*]

[a]*Bundesanstalt für Materialforschung und -prüfung (BAM), Unter den Eichen 87, 12205 Berlin, Germany*
[b]*Laserinstitut Hochschule Mittweida (LHM), University of Applied Sciences Mittweida, Technikumplatz 17, 09648 Mittweida, Germany*

Abstract

X-rays can be generated as an unwanted side effect during ultrashort pulse laser material processing of technical work pieces and even biological samples with laser intensities above 10^{13} W/cm^2. First studies demonstrate the need to address this effect in industrial as well as in medical applications. This secondary hazard should be considered in work safety and risk assessment.

Keywords: ultrashort pulse laser processing; laser-induced X-ray emission; secondary hazard

1. Introduction

Ultrashort laser pulses have become established in many industrial processes (Mottay et al., 2016). Additionally, they are also an integral part of medical applications especially in ophthalmology (Asshauer et al., 2021) and to some extent in dentistry (Rapp et al., 2022). The availability of highly repetitive powerful laser sources and advanced laser beam control systems have favored these developments. However, the laser processing may be accompanied by the generation of unwanted X-rays. Small doses per laser pulse can accumulate to significant dose levels at high laser pulse repetition rates (Legall et al., 2018). Moreover, burst mode laser processing increases the X-ray dose rates compared to single pulse usage (Metzner et al., 2021, Schille et al., 2021) and can result in X-ray photon energies up to 40 keV for tungsten targets (Böttcher et al., 2022). Recently, for laser treatment of human teeth, noticeable X-ray skin dose rates

* Corresponding author. Tel.: +49-30-8104-1822; fax: +49-30-8104-71822
E-mail address: joerg.krueger@bam.de

were found (Kraft et al., 2023). This paper briefly introduces the field of undesired generation of X-ray radiation during ultrashort pulse laser processing in air and directly compares technical and biological materials for processing with an identical experimental configuration.

2. Materials and Methods

For the basic investigations an industrial grade laser source was used inside a fully enclosed machine to protect against primary laser radiation and secondary hazards. The laser source was a near-infrared (NIR) laser (Edgewave FX200, wavelength λ = 1030 nm) and emitted pulses with a duration τ_H of 600 fs. The maximal pulse energy $Q_{P/max}$ was 35 µJ. After a beam expander the laser beam was focused through an aspherical lens (80 mm focal length) to achieve a small focal spot with sufficient working distance (Fig. 1(a)). The tight focusing geometry of the near-Gaussian shaped laser spot was evaluated by a Micro Spot Monitor MSM25 (Primes GmbH) in the range of ± 200 µm around the focal plane z_{foc}. Based on these measurements, the peak intensity I_0 was determined for different positions in the beam caustic. As shown in Fig. 1(b), the peak intensity in the different planes (circles) followed the intensity along the beam waist (dotted line) according to $I(z) \sim 1/\sqrt{[1+(z/z_r)^2]}$, where z_r is the Rayleigh length. The highest peak intensity was in the focal plane of $I_0 = (7.8 \pm 0.4) \cdot 10^{13}$ W/cm^2, decreasing below $2 \cdot 10^{13}$ W/cm^2 at 200 µm defocused position

As a special feature, the laser system could generate pulse trains, or rather laser bursts, with a repetition frequency of f_B = 48.6 MHz of the intra-burst pulses. In this burst-regime at f_P = 5 kHz burst repetition frequency, the average laser power increased linearly with every added pulse in the laser burst, as depicted at the bottom of Fig. 1(a). For example, by irradiating a 2-on-1 burst, consisting of two intra-burst pulses in a laser burst, the average power was 318 mW, increasing either to P_{av} = 455 mW or 581 mW for the 3-on-1 or 4-on-1 laser bursts, respectively. The average power for single pulses at 5 kHz, indicated as 1-on-1 in Fig. 1(a), was P_{av} = 178 mW. The highest investigated average laser power in this study was P_{av} = 890 mW which was irradiated at f_P = 25 kHz in the single-pulse regime (1-on-1).

In addition to the (technical or biological) material, the laser and process parameters strongly influence the laser-induced X-ray emission. In order to process defined areas, the work pieces were moved by an *xy*-axis stage with precise pulse distances of pd = 1 µm at moving speeds between 5 mm/s ≤ v_S ≤ 25 mm/s. According to $v_S = pd \cdot f_P$, this led to comparably low burst repetition frequencies ranging from f_P = 5 kHz to 25 kHz (Fig. 1(a)). At such low repetition rates, potential pulse-to-pulse interactions through heat-accumulation or ablation plasma shielding effects are avoided or at least minimized (“no memory”). Additionally, the thermal

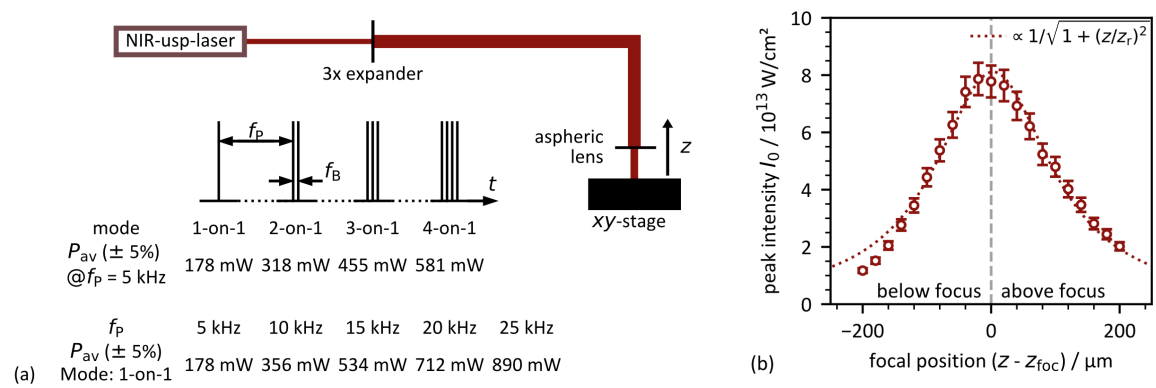

Fig. 1. (a) Experimental setup to generate laser peak intensities up to $8 \cdot 10^{13}$ W/cm^2; (b) laser peak intensity on the sample surface for different *z*-positions of the aspheric lens.

load on the work pieces is reduced. In industrial laser machining, a wide range of materials is used from metals over ceramics to semiconductors. In this study, the chosen technical material was stainless steel AISI 304 (X5CrNi-18-10). For the biological part, water (tap water) and sodium saline solution (0.9 NaCl in water) as a main component of the most biological materials represent models of soft tissue. Besides that, human teeth typify a biological hard material. For better handling the teeth were embedded in epoxy resin and flat grinded at the top.

For the detection of the laser-induced X-rays, a dosimeter (OD-02, Step GmbH) and a spectrometer (SILIX lambda, Ingenieurbüro Prof. Dr.-Ing. Günter Dittmar) were arranged at 15 cm distance to the laser-material interaction point where the laser-induced plasma was generated. The angle to the surface of the materials was adjusted to about 35° to detect a maximal potential X-ray emission (Legall et al., 2018). The natural background radiation was measured inside the laser machine over one hour. A mean X-ray skin dose rate of (80 ± 60) nSv/h was seen.

3. Processing of technical materials

3.1. Influence of intra-burst pulse number

It has been reported so far that laser bursts with intra-burst pulse repetition frequencies ranging from MHz up to the GHz level in combination with high burst repetition frequencies of several hundred kHz strongly affect the laser-induced X-ray dose rates. Here, a comparably low burst repetition frequency of f_P = 5 kHz was used to investigate solely the influence of the intra-burst pulse number N_B on X-ray emission and further to avoid interaction between consecutive bursts. Fig. 2 depicts the measured X-ray skin dose rate vs. laser peak intensity which was varied by changing the focus position of the laser beam relative to the sample surface. For single pulse (1-on-1) and burst (N_B-on-1, $2 \leq N_B \leq 4$) laser processing, both measuring instruments showed an increase of the dose rate with shorter distance between the focal plane and the sample surface. This resulted most likely from the higher peak intensity of the pulses irradiating at substrate positions closer to the focal plane. In addition, it was found that the X-ray dose rate increases with higher number of pulses in a burst which is due to the fact that the average power increased with higher intra-burst pulse number, see Fig. 1(a, bottom). For example, for N_B = 4 (581 mW average power) the skin dose rate $\dot{H}'(0.07)$ was measured of almost 1 mSv/h while less than 0.4 mSv/h was measured for single pulse processing (178 mW average power).

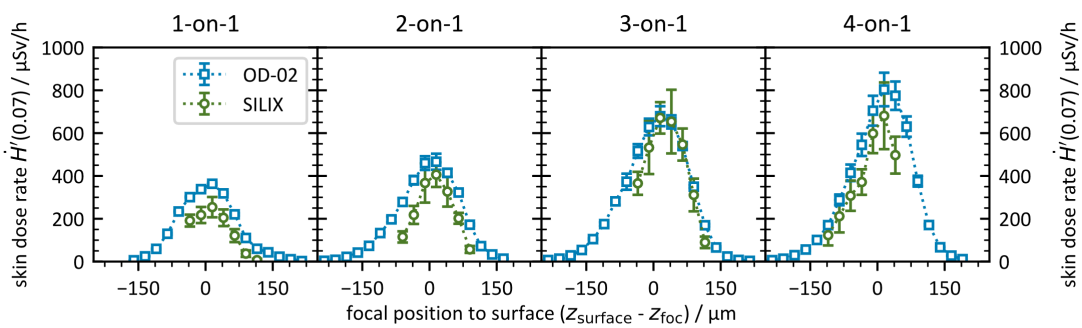

Fig. 2. Measured skin dose rate while processing stainless steel at different distances of the focal plane to the sample surface. The number of pulses in the burst (f_B = 48.6 MHz) increases from left to right. The burst repetition frequency f_P of 5 kHz resulted from the sample translation speed of 5 mm/s and a pulse distance of 1 µm. The errors indicate the 2σ-variation of the dose rates within the process.

3.2. Influence of average laser power

With the above-mentioned assumption of "no memory of previous events" for low repetition rates of the order of 10 kHz, different sample translation speeds can be used to investigate the influence of the average power on the skin dose rate without changing pulse energy and peak intensity. Higher sample translation speeds in combination with higher pulse repetition rates do not modify the single pulse event. With this knowledge, the increase in the sample translation speed should increase the laser-induced X-ray dose rate linearly. As depicted in Fig. 3(a), this behavior can be seen up to the maximal used speed of 25 mm/s at 890 mW and 25 kHz repetition rate. The ratio of skin dose rate and average power $\dot{H}'(0.07)/P_{av}$ is constant and a value of ≈ 1.5 mSv/h/W was found here. In terms of laser energy, an X-ray emission dose level of about 0.4 µSv/J can be calculated which is in good agreement to previous X-ray dose values reported elsewhere (Schille et al., 2021, Legall et al., 2021). Fig. 3(b) shows a plot of the quotient $\dot{H}'(0.07)/P_{av}$ utilizing the data of Fig. 2 of the burst processing with up to four intra-burst laser pulses. Interestingly, also a nearly constant normalized dose rate is found. This can be seen for both X-ray detectors (OD-02, SILIX lambda) which supplied similar skin dose rates within the scope of measurement accuracy of X-ray measurement devices.

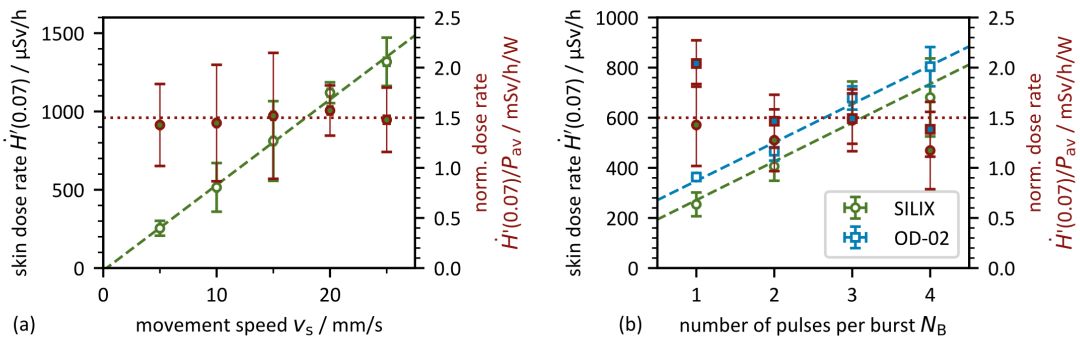

Fig. 3: Influence of the average laser power on the laser-induced X-ray emission at low repetition rates and constant peak intensity for various sample translation speeds and constant pulse distances of 1 µm (a) and number of pulses in the MHz burst (b). The normalized dose rate values are indicated by the red dotted line. The errors show the 2σ-variation of the dose rates within the process.

It must be mentioned that burst processing had no significant effect on X-ray emission in the investigations shown here in contrast to previous research (Metzner et al., 2021, Schille et al., 2021)). In the literature a strong increase of the dose levels in burst mode processing is reported, however, by using much higher average laser powers and burst repetition frequencies.

4. Processing of biological samples

Ultrashort laser pulses are driving an increasingly broad field of applications in medicine, especially in ophthalmology and dentistry. In a recent study (Kraft et al., 2023), X-rays were generated by focusing laser pulses (τ_H = 600 fs, λ = 1030 nm) with intensities up to $8 \cdot 10^{13}$ W/cm² on representative biological materials. The experiments were performed with low average laser power of 178 mW and pulse repetition rates of 5 kHz to minimize thermal load to the biological substrates.

Water and isotonic saline solution as well as porcine eyes (as a model for human eyes) were used as soft tissues or soft tissue substitutes. For these soft tissues, a maximum skin dose rate $\dot{H}'(0.07)$ = 0.8 µSv/h at a detector distance of 15 cm was measured at laser intensities > $5 \cdot 10^{13}$ W/cm². These laser-induced X-ray emissions clearly exceeded the natural background, see Fig. 4. At the same detector distance, X-ray skin dose rates up to 20 µSv/h were monitored on hard dental material that was ground and embedded in epoxy resin before. The start of X-ray emission was detected for the laser treatment of teeth at relatively low laser peak intensities of $2 \cdot 10^{13}$ W/cm².

The skin dose rate and the normalized dose rate are depicted in Fig. 4 as a function of peak intensity. In addition to the biological material, X-ray emissions on stainless steel are presented which were obtained under similar experimental conditions with f_P = 5 kHz in 1-on-1 mode at 5 mm/s sample translation speed, as described above more in detail.

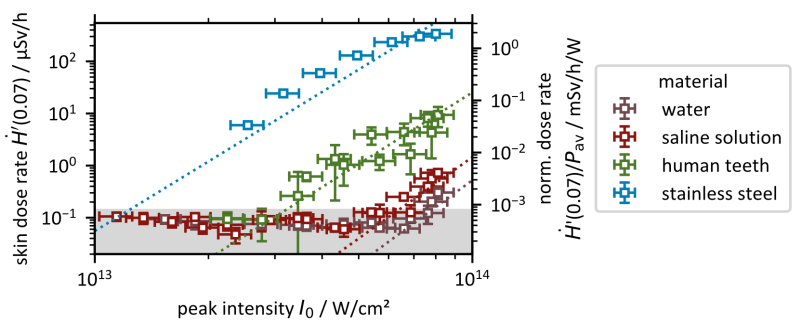

Fig. 4. X-ray skin dose rate for technical and biological materials vs. laser peak intensity. For each material one series of experiments at f_P = 5 kHz with 1-on-1 events is plotted. On the right ordinate normalized dose rate values are given. The dotted lines guide the eye in the log-log plot. The gray area indicates the 2σ-range of the natural background in the lab.

For single pulse stainless steel (AISI 304, X5CrNi-18-10) processing, a maximum skin dose rate of 400 µSv/h was measured at a detector distance of 15 cm for the highest laser peak intensity of about $8 \cdot 10^{13}$ W/cm². For human hard dental material, however, considerably lower dose rates in the order of 10 µSv/h were detected at similar peak intensity level. The soft tissues showed X-ray emission dose rates below 1 µSv/h that is clearly above the 2σ-range of the natural background radiation which is gray marked in Fig. 4.

5. Conclusions

In a fixed experimental setup, X-ray dose rate measurements were performed simultaneously during ultrashort infrared pulse laser treatment (τ_H = 600 fs, λ = 1030 nm) of technical and biological materials. A low laser pulse repetition rate of 5 kHz was used to avoid thermal load of the samples and any "memory" for the following pulse.

Steel as an example for important technical materials shows about one to two orders of magnitude higher X-ray skin dose rates than the biological hard material tooth. Nevertheless, dose rates in the order of 10 µSv/h at 15 cm detector distance for tooth are worth mentioning because of considerable problems to shield from X-ray radiation appearing during laser treatments in the human body at much closer distance.

For steel and at low pulse repetition rates, the laser-induced X-ray emission seems to be more dependent on the peak intensity than on the average laser power. This statement applies to both, the laser treatment with single pulse trains and also to MHz pulse burst machining.

Acknowledgements

The authors gratefully acknowledge financial support by the German Federal Office for Radiation Protection (BfS) under the administrative agreement with contract number 3621S42451.

References

Asshauer, T., Latz, C., Mirshahi, A., Rathjen, C.. 2021. Femtosecond lasers for eye surgery applications: historical overview and modern low pulse energy concepts. Advanced Optical Technologies 10, p. 393.

Böttcher, K., Schmitt Rahner, M., Stolzenberg, U., Kraft, S., Bonse, J., Feist, C., Albrecht, D., Pullner, B., Krüger, J. 2022. Worst-Case X-ray photon energies in ultrashort pulse laser processing. Materials 15, p. 8995.

Kraft, S., Schille, J., Bonse, J., Löschner, U., Krüger, J. 2023. X-ray emission during the ablative processing of biological materials by ultrashort laser pulses. Applied Physics A 129, p. 186.

Legall, H., Schwanke, C., Pentzien, S., Dittmar, G., Bonse, J., Krüger, J. 2018. X-ray emission as a potential hazard during ultrashort pulse laser material processing. Applied Physics A 124, p. 407.

Legall, H., Bonse, J., Krüger, J. 2021. Review of X-ray exposure and safety issues arising from ultra-short pulse laser material processing. Journal of Radiological Protection 41, p. R28.

Metzner, D., Olbrich, M., Lickschat, P., Horn, A., Weißmantel, S. 2021. X-ray generation by laser ablation using MHz to GHz pulse bursts. Journal of Laser Applications 33, p. 032014.

Mottay, E., Liu, X., Zhang, H., Mazur, E., Sanatinia, R., Pfleging, W. 2016. Industrial applications of ultrafast laser processing. MRS Bulletin 41, p. 984.

Rapp, L., Madden, S., Rode, A.V., Walsh, L.J., Spallek, H., Nguyen, Q., Dau, V., Woodfield, P., Dao, D., Zuaiter, O., Habeb, A., Hirst, T.R. 2022. Anesthetic-, irrigation- and pain-free dentistry? The case for a femtosecond laser enabled intraoral robotic device. Frontiers in Dental Medicine 3, p. 976097.

Schille, J., Kraft, S., Pflug, T., Scholz, C., Clair, M., Horn, A., Loeschner, U. 2021. Study on X-ray emission using ultrashort pulsed lasers in materials processing. Materials 14, p. 4537.